

Enhanced removal of Cr(III), Mn(II), Cd(II), Pb(II) and Cu(II) from aqueous solution by N-functionalized ordered silica

Natalia Kobylinska

Taras Shevchenko National University of Kyiv, 64/13, Volodymyrska Str., Kyiv, Ukraine, 01601

<https://orcid.org/0000-0001-8181-1451>

Vadim Kessler

Department of Molecular Sciences, Swedish University of Agricultural Sciences, 75007 Uppsala, Sweden

<https://orcid.org/0000-0001-7570-2814>

Gulaim Seisenbaeva

Department of Molecular Sciences, Swedish University of Agricultural Sciences, 75007 Uppsala, Sweden

<https://orcid.org/0000-0003-0072-6082>

Oksana Dudarko (✉ odudarko80@gmail.com)

Chuiko Institute of Surface Chemistry of NAS of Ukraine, 17 General Naumov Str., Kyiv, Ukraine, 03164

<https://orcid.org/0000-0002-8353-8089>

Research Article

Keywords: Functionalization, Heavy metals, Simultaneous determination, Isotherms, Removal

Posted Date: February 3rd, 2021

DOI: <https://doi.org/10.21203/rs.3.rs-196968/v1>

License:  This work is licensed under a Creative Commons Attribution 4.0 International License. [Read Full License](#)

Abstract

Chelating and ion-exchange N-functionalized mesoporous silicas (SBA-15) as selective adsorbents for removal of heavy metals were synthesized using template method. Fourier transform infrared spectroscopy, TEM analysis, N₂ adsorption/desorption isotherms and titration analysis confirmed successful functionalisation of the tri-sodium salt of N-(triethoxysilylpropyl)ethylenediaminetriacetic acid (EDTA), protonated primary amine (NH₃⁺Cl⁻) and its combinations onto the mesoporous silica (SBA-EDTA/NH₂). The obtained materials featured beneficial properties of mesoporous silica SBA-15 with its high surface area and were successfully fictionalized with N-containing groups. The synthesized series of silicas were investigated for removal of Cr(III), Mn(III), Pb(II), Cd(II) and Cu(II) from model water solutions. The adsorption of target ions increased with the increase pH and its concentration in solution. The adsorption equilibrium data were well fitted to Langmuir isotherm model and maximum monolayer adsorption capacities for cations Pb(II), Cd(II), Cr(III) and Mn(II) were 185.6 mg g⁻¹, 111.2 mg g⁻¹, 57.7 mg g⁻¹ and 49.4 mg g⁻¹, respectively. The chelating interaction was considered as the main adsorption mechanism for metal ions (Cr(III), Mn(II), Pb(II), Cd(II), and Cu(II)). The adsorption capacities of SBA-EDTA and SBA-EDTA/NH₂ samples toward studied metal ions were consistent with the Lewis 'hard and soft acids and bases' theory. The metal removal efficiency of adsorbents was near 96-92 % during three regeneration cycles. All these results indicated that the produced N-functionalized silica were promising for applications in environmental and analytical separation fields.

1. Introduction

The rapid industrialization, consumer lifestyles, accumulation of Life-of-End products, development of electroplating, metallurgy sludge, newspapers printing, synthetic dyeing and electronics processing industries, the damage caused by heavy metal pollution to the environment water medium is becoming more and more problematic moments [[1], [2]]. Pollution occurs both at the level of industrial production and at the Life-of-End products:

- Chromium (Cr) – mining, industrial coolants, production of chromium salts, tanned leather, cement, metal finishing, leather tanning, electroplating, paints, and also the metal finishing discharge;
- Lead (Pb) – lead-acid batteries, printing paints and colorant pigments, electronics waste, smelting operations, coal-fired thermal power plants, ceramics;
- Copper (Cu) – mining, electrical wiring, galvanic process, smelting operations;
- Cadmium (Cd) – zinc smelting, used batteries and accumulators, electronic waste, paints, fuel combustion [[3], [4]].

Also, the heavy metal ions in environmental samples are restricted by some main problems for human healthy. They come to the reservoirs from the environment – from rocks, soil erosion, precipitation, ashes of forest fires, etc. [[5]]. Depending on the geochemical conditions, there are wide fluctuations in their content. As the pH of the water drops, the solubility of the metals increases and the metal particles become more mobile. Therefore, metal ions are more toxic in soft and acidic natural waters. Metals can settle in bottom sediments, where they are stored for many years. Streams from drainage mines are often very acidic, contain high concentrations of dissolved metals and are almost unsuitable for living organisms. They are harmful to the environment because they contain heavy metal ions, which are not subject to biodegradation. Unlike some organic contaminants, such as

organochlorine or organophosphorus pesticides, metal ions cannot degrade into less harmful components under natural conditions [6].

In general, ionic forms of metals are more toxic because they can form toxic compounds with other ions. Once in the reservoir, they are included in the cycle of substances and undergo various transformations. Inorganic compounds are rapidly bound to the water buffer system and converted to sparingly soluble hydroxides, carbonates, sulfides, and phosphates, and form organometallic complexes that are adsorbed by bottom sediments. In addition, heavy metals are dangerous because, as a rule, they bioaccumulated, i.e. accumulate chemicals in the biological organism (also, human body) over time, which is significantly higher than its typical content compared to the concentration of the chemical in the environment. Compounds accumulate in living things every time they enter the body and are stored longer than they are decomposed (metabolized) or excreted from the body [7, 8]. Toxicity of heavy metals can lead to damage to the central nervous system, as well as damage to the blood, lungs, kidneys, liver and other vital organs [9, 10].

The heavy metals ions can be extracted from water by different methods. The trace level of concentration of metal ions in environmental aqueous medium is a major problem in the instrumental detection of heavy metal ions by various methods, including atomic absorption spectrometry, inductively coupled plasma atomic emission spectroscopy and mass spectrometry [11]. Adsorption–pre-concentration systems based on precipitation [12], liquid–liquid extraction [13], cloud point extraction [14], membrane filtration [15] are used to solve this problem. However, most of the used sample preparation methods have certain disadvantages, such as incomplete ion extraction, expensive, energy consumption, high amount of sludge and low selectivity [16]. Separation and pre-concentration of trace metal ions by solid phase extraction are also widely used for that purpose [17]. In these techniques, suitable, selection of adsorbent is crucial to ensure quantitative retention of the toxic compounds and, in some cases, selective adsorption. Silica and activated carbons are widely used to remove toxic substances from wastewater. In these methods, the appropriate choice of adsorbent is crucial to ensure the quantitative removal of toxic compounds and, in some cases, selective adsorption. Organo–inorganic materials and activated carbon are widely used adsorbents to remove toxic substances from wastewater. Recent reviews showed that organic–inorganic mesoporous materials possessed great potential to be excellent adsorbents for the heavy metal ions [18, 19]. Bonding the target selective functional groups to the silica surface by ‘one-pot’ condensation or grafting post-synthesis approach has been used to create specific active sites in the mesopores channels of these materials. Because the amine group is capable of interacting with cationic, anionic and/or neutral pollutants from aquatic environments [20, 21, 22], a lot of attention was paid to this class of sorbents. Among these functional groups, amine modification with more active centre being introduced could effectively enhance the adsorption capacity [23, 24]. Wei et al. showed greatly improved adsorption performance towards Cu(II) ions due to the higher amount of N-containing functional groups on the surface of the adsorbent [25]. Adsorbents with functional groups of primary and secondary amines exhibit both complexing properties with respect to transition metal ions and ion-exchange properties with respect to their anionic complexes [26, 21]. An increase in the number of binding sites in functional groups due to an increase in the number of nitrogen atoms could lead to an increase in the stability constants of surface complexes with heavy metal cations, a decrease in or elimination of the stepwise complexation, and an increase in the adsorption capacity of the adsorbent. The high adsorption removal efficiency of heavy metal ions was observed using polyamine-[27] or melamine-based dendrimer amines [28] functionalized mesoporous silica. An increase in the stability constants can be accompanied by an increase in the difference between these constants for different metal ions, that is, an increase in the separation selectivity when using a pH gradient [24]. In addition to the aforementioned, also chelate groups have attracted considerable

attention, especially in the field of separation of various toxic metals in mixture [[29]]. Ethylenediaminetetraacetic acid (EDTA) is favourable N,O-containing agent for modified adsorbents with chelating and ion-exchange properties for many different metal ions, for example, Pb(II) [[30]]. The review of literature presented in this paper demonstrates good potential of N-containing ligand-functionalized silica based materials for the selective extraction and separation of heavy metal ions in cationic forms from aqueous solution by adsorption. In fields of solid supports, SBA-15 material has the unique parallel cylindrical pores hexagonal ordered and high specific surface areas that suggesting a high adsorption capacity of adsorbent and effective mass transfer for fast adsorption equilibrium. The novel idea of our work is the use of template method for the synthesis of SBA-15-based adsorbents with uniform distribution of functional groups. The combining several N-containing functional groups with various mechanism of interact can also change the connecting sites in order to enhance the removal of metal ions in a wider pH range.

In the present work, we used the SBA-based adsorbent approach to make a compiled and comparative study of different N-containing groups (N-(triethoxysilylpropyl)ethylenediaminetriacetic acid (EDTA), primary amine (NH_3^+Cl) and its combinations. In order to improve the selective adsorption by proposed materials, a different functionalizing technology was employed, offering a potentially powerful method for selective adsorption of series bivalent (*Mn(II)*, *Pb(II)*, *Cd(II)*, *Cu(II)*) and polycharged (*Cr(III)*) heavy metal ions from water solutions as target species. The mesoporous silica was used as an effective adsorbent for extraction of heavy metal ions with subsequent determination by the atomic absorption spectrometry (AAS). The removal of heavy metals on modified mesoporous silica samples was investigated by batch adsorption experiment including investigation of pH influence, adsorption isotherms and mechanisms, etc.

2. Material And Methods

2.1. Chemicals.

Sodium metasilicate ($\text{Na}_2\text{SiO}_3 \cdot 9\text{H}_2\text{O}$, SS), aminopropyltriethoxysilane (APTES, 98%), 3-aminopropylsilanetriol (Gelest, 22-25% in water), trisodium salt of N-(triethoxysilylpropyl) ethylenediaminetriacetic acid (EDTA, 40% in water) were obtained from Sigma-Aldrich USA, tetraethoxysilane (TEOS, 99%) – from Fluorochem. All inorganic reagents were of analytical grade ($\text{Cu}(\text{NO}_3)_2 \cdot 5\text{H}_2\text{O}$, $\text{Fe}(\text{NO}_3)_3 \cdot 9\text{H}_2\text{O}$, $\text{Cd}(\text{NO}_3)_2 \cdot 4\text{H}_2\text{O}$, $\text{Cr}(\text{NO}_3)_3 \cdot 9\text{H}_2\text{O}$, K_2CrO_4 , $\text{Mn}(\text{NO}_3)_2 \cdot 6\text{H}_2\text{O}$, KMnO_4 and $\text{Pb}(\text{NO}_3)_2$). The working solutions were prepared with deionized water ($18.2 \text{ MW} \cdot \text{cm}^{-1}$).

2.2. Synthesis of adsorbents.

Synthesis of SBA-EDTA. The material was prepared following reference [[31]] with several modifications. Briefly, Pluronic P123 (2 g) was dissolved in 30.0 mL of 2 M HCl and 10.8 mL of distilled water was added during 3.5 h under rapid stirring at 40 °C. Next step, 4.4 mL (0.02 mmol) of TEOS was added dropwise under stirring to the reaction mixture at 40 °C. After half an hour, about 10 mL of TMS-EDTA solution in methanol (1:1) was added to synthesis gel and stirred for 24 hours at 80 °C under hydrothermal conditions. The precipitate was separated by filtration and washed by ethanol/HCl mixture several (3-4) times during 24 hours. In this stage, functional groups of SBA-EDTA sample were converting to H-form. Finally, SBA-EDTA sample was decanted and washed with deionized water until neutral pH, and thereafter dried under vacuum at 80 °C.

Synthesis of SBA-NH₂. The 3.2 g of P123 were dissolved in 32 mL of deionized water on constant stirring at room temperature. Then, 29.4 mL of concentrated hydrochloric acid were added to the clear solution. 0.36 mL APTES were added by drops to the solution of surfactant. After 5 min without interrupting the stirring, 6.8 g SS dissolved in 32 mL of water were added to the transparent mixture on continuous stirring at room temperature. After precipitation, the sample was stirred for 2 hours at 40 °C. Hydrothermal treatment was carried out (20 hours at 80 °C). After drying, the sample was refluxed in ethanol (30 cm³ per 1 gram) 4 times for 3 hours. Dried 0.5 hour at RT, 0.5 hour at 50 °C, 3 hours at 100 °C.

Synthesis of SBA-EDTA/NH₂. 4 g P123 were dissolved in 40 mL of deionized water on constant stirring at room temperature. Then, 32 mL of concentrated hydrochloric acid were added to the transparent solution. Then 1.85 mL (0.002 mol) EDTA and 1.18 mL (0.002 mol) APTS at room temperature were added by drops without stop stirring. The clear solution of 4 g SS in 40 mL of deionized water was added to the mixture on continuous stirring at room temperature. Other steps of the treatment were the same to the abovementioned technique.

2.3. Characterization.

Fourier transform infrared spectra (FTIR) of all samples were recorded using the KBr pellet technique (1:20). The FTIR spectrophotometer (Nicolet NEXUS 470) was used in the range 400-4000 cm⁻¹. Transmission electron microscope (TEM, SELMI PES-125K) was used to prove the structure and morphology of the mesoporous samples. Textural properties of the mesoporous matrices were determined from the N₂ adsorption/desorption isotherms recorded at 77 K with a Kelvin-1042 apparatus (Costech Instruments, USA). Specific surface area (S_{BET}) and pore diameter of the samples was determined by the BET [\[\[32\]\]](#) and the BJH [\[\[33\]\]](#) methods, respectively.

Concentrations of functional groups on the mesoporous silica surfaces were determined by pH-metric titration (I-160M). A batch of the sample with protolytic active groups (~0.05 g) was poured with 25 mL of 0.1 M NaNO₃, incubated for 24 hours, and titrated with 0.1 M NaOH solution.

Atomic absorption spectrometer equipped with fast sequential mode (iCE 3500, Thermo Scientific, USA) was used for analytes concentrations determination. The diffuse reflectance spectra were recorded using Thermo Scientific *Evolution 600 Spectrophotometer* designed to hold solid samples for transmittance measurements.

2.4. Metal Uptake Experiments.

A 50 mg sample of functionalized silica was shaken with 25 mL of 0.02 M of aqueous solution of the appropriate metal ions (Mn(II), Cr(III), Cd(II), Pb(II) and Cu(II)) solution using 50 mL glasses. Initial pH of the suspension to the equilibrium value for these experiments were adjusted by HCl or NaOH and controlled with a pH meter. The suspensions were mechanically shaken overnight. Then, the suspensions were centrifuged for 10 min at 1500 rpm. The supernatant was analyzed for the amount of metal ions by AAS. Each study was performed at least in a triplicate.

Adsorption isotherms were investigated for estimation of the maximum adsorption capacities of the obtained adsorbents. Adsorption experiments were carried out by adding 0.05 g samples into 25 mL of various concentrations of each metal solution (50, 100, 200, 300 and 400 mg/L) at room temperature. The suspensions were mechanically mixed overnight at controlled pH, optimal for each metal. Then, the suspensions were centrifuged (10 min) and the liquid phase was analyzed by AAS.

Determination of the metal ion concentration was carried out by allowing the insoluble complex to settle down and appropriate volume of the supernatant was withdrawn using a micropipette then diluted to the linear range of the calibration curve for each metal.

2.5. Desorption study.

The adsorbents were regenerated in 15.0 mL centrifuge tubes with 5.0 mL of different leaching solutions (HNO₃, EDTA) at room temperature for 0.5-3 hours. The effects of concentration and volume of the optimal leaching solution on desorption efficiency were also investigated.

3. Results And Discussion

3.1. Adsorbents synthesis strategy.

For producing N-containing functional mesoporous silicas, we could choose three different cases, (1) chelating agent with tertiary N and carboxylic groups (SBA-EDTA), (2) low ion-exchange agent with protonated aminopropyl groups (SBA-NH₂), or (3) amphoteric poly-functional agent with combination of chelating and low ion-exchange groups (SBA-EDTA/NH₂). Different surface groups of synthesised silica are schematically shown in **Figure 1**.

The mesostructure ordering and symmetry was confirmed by the TEM data (**Fig. 2**). The 2D-*P6mm* hexagonal symmetry with a diameter of about 7.0 nm could clearly be observed in all samples.

The chemical functionality of a series of obtained mesoporous samples was controlled by FTIR spectroscopy (**Fig. 3a**). Using a titration experiment by acid-base interactions, the amount of functional groups in the samples was quantified (**Fig. 3b**).

The characteristic vibration bands of SBA-15 ($\nu_s(\text{OH})$, 3440 cm⁻¹; $\nu_{as}(\text{Si-O-Si})$ at 1080 cm⁻¹ and $d(\text{Si-O-Si})$ at 798 cm⁻¹, $d(\text{Si-OH})$, 961 cm⁻¹) are displayed in the all FTIR spectra. Also, the symmetric and asymmetric flexible alkyl groups vibrations with different intensity ($\nu_{as}(\text{C-H}) = 2925 \text{ cm}^{-1}$ and $\nu_s(\text{C-H}) = 2855 \text{ cm}^{-1}$) was witnessed. The band at 1723 cm⁻¹ (corresponding to $\nu(\text{C=O})$ of COOH groups) of EDTA functionality of SBA-EDTA sample are displayed (**Fig. 2b**). For *SBA-EDTA/NH₂* an absorption band characteristic for the bending vibrations of protonated primary aminoalkyl groups $\delta_s(\text{NH}_3^+)$ at 1582 cm⁻¹ [[34]] was identified, while the band corresponding to $\delta_{as}(\text{NH}_2)$ was masked by the absorption band of water $\delta(\text{H}_2\text{O})$ at 1625-1630 cm⁻¹. The very broad $\nu_s(\text{OH})$ peak of hydrogen bonded Si-OH around 3400 cm⁻¹ masked the low band of $\nu(\text{N-H})$ at 3245 cm⁻¹ of functionalized samples. From these results, it can be concluded that organic moieties are indeed bound to the SBA-15 matrix. The specific surface area, total pore volume and pore size of the samples from N₂ adsorption/desorption isotherms were estimated using BET equation and BJH method; and values are summarized in **Table 1**.

Table 1. Textural and quantitative parameters of functionalized mesoporous samples derived from N₂ adsorption/desorption isotherms and potentiometric titration data, respectively.

Sample	N ₂ isotherms		Potentiometric titration	
	S _{BET} (m ² •g ⁻¹)	V _{total} (cm ³ •g ⁻¹)	d (nm)	C _L (mmol•g ⁻¹)
SBA-EDTA	745	1.44	6.2-7.4	0.95
SBA-NH ₂	700	0.99	6.6	0.11
SBA-EDTA/NH ₂	710	1.03	6.6	0.10/0.32

Notes: S_{BET} – Surface area calculated by method BET, V_{total} – volume of adsorbed N₂ at p/p₀=0.93, d – diameter pores calculated by BJH, C_L – concentration of ligands.

The specific surface areas of only NH₂-groups or EDTA factionalized SBA-15, and its mixture factionalized mesoporous silica were 700, 745 and 710 m²•g⁻¹, respectively. Thus, the multicomponent nature of the reaction mixture does not affect the texture parameters of the functionalized sample. The pore diameter was around 6.6-7.4 nm, which was in agreement with the TEM analysis (Fig. 2).

Quantitative determination of the protolytic-active functional groups was measured by pH-metric titration (**Fig. 3b**). The most gradual change is the curve of the pH-metric titration was observed for *SBA-EDTA*, explained by the presence of zwitter-ionic interactions on the surface of the silica [[35]] and high concentration of the functional groups (**Table 1**). When the N-containing groups were bounded on the silica dioxide surface, their pK decreased, and this effect was enhanced in the case of amphoteric zwitter-ion groups, which also affected the smoothness of pH change during titration of such materials. In addition, acid-base interactions of N-containing groups and residual silanol groups contributed to a smooth change in the pH range 4-9 [[36]].

3.2. Influence of initial pH on adsorption of metal ions.

The adsorption capacity of the adsorbent in relation to the uptake of heavy metals is dependence by many factors, including the properties of the metal ions themselves, such as the atomic radius and oxidation state, concentration in aqueous solution and experimental conditions. The pH of the aqueous solution is probably the most important parameter influencing the adsorption process, especially for samples functionalized with protolytically active groups.

Therefore, the sorbents functionalized with N-containing groups usually show the dependence of their complexing properties on pH [[37]]. Figure 4 shows the effect of pH on the adsorption of metal ions by representative mesoporous silicas.

The N-containing silicas did not adsorb any of the metals studied when the pH of solutions was less than 2 (**Table 2**). The maximum removal of Cr(III), Cu(II) ions on *SBA-EDTA/NH₂* increased to pH 4.3 while for Mn(II) and Pb(II), it

was maximized at 6.0 (**Fig. 4**). The least stable complexes on the surface of adsorbents were formed by Mn(II) - that adsorbed at pH 3-6, while Cu(II) and other metals were desorbed at pH 2.5-4.0. As the pH of the medium increased when studying the sorption of Cu(II) ions, the adsorbents were stained blue. The most intense color was observed for the *SBA-NH₂* sample. The effect of Cu(II) in the surface silica was studied by UV-Visible *spectroscopy of diffuse reflectance* (**Fig. 5**).

The diffuse reflectance spectra were observed maximum at 640 nm (15620 cm^{-1}). This is characteristic of metal-to-ligand charge transfers in Cu(II) complexes [[38]]. The dependence of the analytical signal on the Cu(II) ions in silica surface was increased in the range pH 2.5-4.5. Under acidic conditions the N-atoms are protonated and do not participate in coordination of Cu(II) ions (**Fig. 5**). At increasing pH the formation of N,O-chelating ring can be excluded. At pH close to neutral, the sedimentation of Cu(II) ions is observed, as evidenced by the disappearance of the absorption band in the spectrum. From the above *diffuse reflectance* spectra, we can summarize that when *SBA-EDTA/NH₂* is loaded with Cu(II) ions, ion adsorption could involve interactions between metal complexes and deprotonated silanol groups or organic motives. The EDTA⁻ and aminogroups of *SBA-EDTA/NH₂* sample could interact with Cu(II) ions via chelating effect like silica with NH₂-groups [35].

The order of sorption of transition metals on each sorbent is generally consistent with the stability constants of complexes of transition metals with the surface ligands, EDTA⁻ and NH₂-groups [[39]]. The complexing properties of the mono-functionalized adsorbent, since the functional groups within the cycle will be represented by only one type of groups. However, when silica is modified with EDTA and amino groups, the oxygen atoms will also be present in the cycle, which, given their location, will probably affect the increase in the sorption capacity and the selectivity of the sorbent with respect to Cd(II) and Cr(III), since in this case these transition metals will be retained due to heteroligand chelates of functional groups.

3.3. Adsorption isotherm and complexation of metal ions.

The adsorption isotherms were applied to characterize the interaction of several the most reprehensive heavy metal ions with the obtained adsorbent, by expressing the relation between the amount of target ions uptake and remaining metal ion concentration in water solution at equilibrium state. Isotherm adsorption measurements were carried out by the static method (**Fig. 6**).

The adsorption isotherms show a sharp initial slope, indicating that both materials acted as highly efficient adsorbents at low metal concentrations (Fig. 6). It was obvious that bi-functionalization (*SBA-EDTA/NH₂* sample) was enhancing the adsorption affinity of adsorbent. According to the isotherms of *SBA-EDTA* sample, the adsorption capacities were about $185.6\text{ mg}\cdot\text{g}^{-1}$ for Pb(II), $111.2\text{ mg}\text{ g}^{-1}$ for Cd(II), $57.7\text{ mg}\cdot\text{g}^{-1}$ for Cr(III) and $49.4\text{ mg}\cdot\text{g}^{-1}$ for Mn(II). These data demonstrated that the adsorption capacity of obtained materials increased with increasing equilibrium concentration of the metal ions in solution, progressively saturating the adsorbent. Maximum values of the adsorption capacity obtained from the adsorption isotherms for each metal ions agreed with the concentration of functional groups (Table 1). At least four functional groups with donor properties are spatially arranged in such a way that they can usually form 1: 1 complexes. Therefore, the formation of monodentate or hydroxyl complexes of metal ions with functional groups on surface SBA-15 is more favorable than bidentate. One can assume that the bi-functional adsorbent (*SBA-EDTA/NH₂*) forms chelated metal-complex

with six-coordinating metal sit, involving two imino-groups nitrogen atoms, three carboxylic oxygen atoms of EDTA and one nitrogen of a NH_2 -group. At the same time, the monofunctionalized EDTA-SBA material containing the EDTA ligand forms five coordinate metal complex through two nitrogen atoms of imino group and three carboxylic oxygen atoms produced by deprotonation.

The adsorption capacities were higher for Pb(II), and Cd(II), the affinity of the adsorbent *SBA-EDTA/NH₂* following the common order Pb(II) > Cd(II) > Cr(III) > Mn(II). This result is in agreement with the report [[40]]. According to the 'hard and soft (Lewis) acids and bases' (HASB) theory [[41]], the Cr(III) ion with high charge and small radius is a kind of hard acid, which may bond a hard base strongly. The divalent metal ions, which are on the borderline (intermediate) should have different affinities for O and N donor atoms of the EDTA functional group as hard ligand. Also, NH_2 -functional group is considered as hard ligand, which was known to have good protonation ability. Polarization will play an important role in the interaction between metal ions and the ligands when they are in the same valence. The larger the metal ion radius is, the greater the polarization will be. So, the adsorption capacities of *SBA-EDTA* and *SBA-EDTA/NH₂* samples toward studied metal ions are consistent with the HASB theory.

For comparison, the capacities obtained by Faghihian et al. [38] for adsorption of lead(II) and cadmium(II) cations using expanded aminefunctionalized MCM-41 were $169.49 \text{ mg}\times\text{g}^{-1}$ and $64.93 \text{ mg}\times\text{g}^{-1}$, respectively. Shahbazi et al. [28] have obtained $94,8 \text{ mg}\times\text{g}^{-1}$ for lead(II) with melamine-based NH_2 dendrimer modified SBA-15 matrix. The guanidine functionalized adsorbent demonstrated maximum adsorption capacity, 289.9 mg g^{-1} for Pb(II), 259.9 mg g^{-1} for Hg(II) and 228.8 mg g^{-1} for Cd(II) from aqueous medium [27]. Our series of adsorbent has thus shown the one of the highest adsorption capacities for heavy metal ions among the related materials.

To obtain an optimized adsorption system for the extraction of metal ions, it is important to establish the most description for the adsorption equilibrium isotherms. Different isotherm equations were used to describe the equilibrium adsorption characteristic. Various isotherm equations were used to describe the equilibrium characteristics of adsorption. It is well known that Langmuir, Freundlich and Dubinin–Raduskevich models can be used to describe adsorption isotherm [[42], [43], [44]]. Langmuir model assumes that the adsorption of analytes occurs in a monolayer by chemisorption, uniform and limited coverage on the surface of the adsorbent, and the adsorption energy decreases and when removed from the surface. In contrast to the Langmuir adsorption model, Freundlich adsorption model describes the inhomogeneous adsorption behavior of the analyte, in which the adsorption coating of the surface can significantly exceed the monolayer. The adsorption of metal ions was fit to Langmuir, Freundlich, and Dubinin–Radushkevich isotherms using equations representing each model (Fig. 7).

The observed dependences were consistent and predictable among each of the adsorption models for *SBA-EDTA/NH₂* and *SBA-EDTA* samples (Table 2).

Table 2. Fitting parameters obtained by processing linearized adsorption isotherms of different mesoporous samples.

Ions	q_{exp} ($mg\ g^{-1}$)	Langmuir isotherm model			Freundlich isotherm model			Dubinin-Raduskevich isotherm model		
		q_m ($mg\ g^{-1}$)	K_L ($L\ \mu g^{-1}$)	R^2	K_F^*	n	R^2	q_m ($mg\ g^{-1}$)	E, ($kJ\ mol^{-1}$)	R^2
<i>SBA-EDTA/NH₂</i>										
Cd(II)	59.1	60.98	0.10	0.9988	35.76	10.99	0.9968	57.56	9.2	0.8979
Pb(II)	103.5	107.53	0.07	0.9997	34.54	4.97	0.9337	94.51	16.0	0.8118
Mn(II)	36.1	37.74	0.10	0.9981	14.16	5.51	0.9707	32.06	8.0	0.6812
Cr(III)	40.2	43.86	0.03	0.9827	10.72	4.24	0.9522	35.01	8.1	0.8488
<i>SBA-EDTA</i>										
Cd(II)	111.2	112.36	0.11	0.9975	17.93	2.67	0.7045	91.82	10.5	0.9596
Pb(II)	185.6	188.68	0.24	0.9997	54.43	3.56	0.6903	156.62	10.0	0.9277
Mn(II)	49.4	50.00	0.13	0.9977	8.37	2.78	0.7082	41.78	7.1	0.9596
Cr(III)	57.7	60.98	0.09	0.9976	7.51	2.24	0.7980	45.06	9.2	0.9184

Note. $*K_F$ ($mg^{1-1/n}\ L^{1/n}\times g^{-1}$).

It can be seen from Table 2 shows that all three models justifiably coincide with the experimental data. The adsorption data were precisely described by the Langmuir isotherm model and the maximum single-layer adsorption capacity for cationic forms of metals was calculated. The Langmuir model gives better correlation coefficients ($R^2 > 0.99$) and much closer saturated capacity to the experimental value (Table 2), suggesting that monolayer and uniform sorption mode is more appropriate to explain the sorption of metal ions in *SBA-EDTA* and *SBA-EDTA/NH₂* samples. And both the large value of K_L from Langmuir model and the n value of between 1 and 10 from Freundlich model clearly imply strong bonding of metal ions to the *SBA-EDTA/NH₂* adsorbents. The adsorption equilibrium data for *SBA-EDTA* were well fitted to Langmuir isotherm model and Dubinin-Raduskevich model with $R^2 > 0.91$. In addition, mean free energies (E) of 8.0-16.0 $kJ\ mol^{-1}$ were obtained from the Dubinin-Raduskevich model. It is known that the numerical value of E in the range of 1–8 and 9–16 $kJ\ mol^{-1}$ predicts physical and chemical sorption, respectively. That is, the value of E obtained for the adsorbents studied in this work clearly indicates that the adsorption of metal ions in *SBA-EDTA/NH₂* and *SBA-EDTA* samples is chemical adsorption, i.e. chemisorption. These data are consistent with the results obtained for SBA-16 materials with similar functional groups [27].

Indeed, the chemical nature of the interaction is in fact well consistent with the monolayer and uniform adsorption of the target analytes by the Langmuir model, as well as our assumptions that metal ions are removed by complexation with the EDTA or aminopropyl group on the mesoporous adsorbent surface.

3.4. Regeneration ability of adsorbents.

The recycling and regeneration of adsorbents is a key aspect for future practical application. The reusability of thus obtained mesoporous adsorbents was tested using 1 M HNO_3 as eluent (5 mL) with 30 min contact time. The metal removal efficiency by N-containing silicas were near 96-92 % during three regeneration cycles. The significant decrease in adsorption capacity (recovery 80 %) was observed after three consecutive cycles of acid treatment. Relatively complicate desorption of metal ions from the surface of adsorbents originating from strong bonding to functional groups with formation of inner sphere of complexes cause difficulty to remove metal ions from the surface by changing the pH.

Conclusions

This work developed a highly practically valuable adsorption process based on the novel mesoporous materials with N-containing functional groups. They were synthesized for the removal of heavy metals from actual water medium. The materials retained their structural features, i.e. the highly ordered structure and high surface area ($700\text{-}745\text{ m}^2\text{ g}^{-1}$) with the functional ligand content reaching from 0.1 to 0.95 mmol g^{-1} . The study outcomes also demonstrated that *SBA-EDTA/NH₂* had enough potential toward capture of transition metal ions including Cr(III) from aqueous medium. Investigation of isotherms study revealed that the adsorption Cr(III) onto *SBA-EDTA/NH₂* was dominated by monolayer adsorption with high adsorption capacity under neutral pH condition (pH 6). The adsorption isotherms were better fitted to the Langmuir model, indicating the formation of metal ions monolayer covering on the surface of mesoporous adsorbents. The metal removal efficiency by obtained N-containing mesoporous silicas were near 96-92 % during three regeneration cycles. Thus grafting of various N-containing groups onto silica provides a good strategy for removal of the heavy metal ions including toxic chromium (III) and manganese (II) ions from aqueous solutions.

Declarations

Acknowledgments

Authors are grateful to the MES of Ukraine (project M/10-2020) and project "Multifunctional hybrid adsorbents for water purification" supported by the Swedish Research Council (Vetenskapsrådet) Swedish Research links Program, Dnr. 2018-2021.

Declaration of interests

The authors declare that they have no known competing financial interests or personal relationships that could have appeared to influence the work reported in this paper.

References

- [1] Pradel M, Aissani L, Villot J, Baudez JC, Laforest V (2016) From waste to added value product: towards a paradigm shift in life cycle assessment applied to wastewater sludge – a review. *J. Clean. Prod.* 131: 60–75. doi:10.1016/j.jclepro.2016.05.076 75.
- [2] Zhou C, Ge S, Yu H, Zhang T, Cheng H, Sun Q, Xiao R (2018) Environmental risk assessment of pyrometallurgical residues derived from electroplating and pickling sludges. *J. Clean. Prod.* 177: 699–707. <https://doi.org/10.1016/j.jclepro.2017.12.285>
- [3] Islam S, Ahmed K, Raknuzzaman M, Habibullah-Al- Mamun, Kamrul M (2015) Heavy metal pollution in surface water and sediment: A preliminary assessment of an urban river in a developing country. *Islam Ecol. Indicators*, 48: 282-291. <https://doi.org/10.1016/j.ecolind.2014.08.016>
- [4] Cegłowska M, Gierczyka B, Frankowska M, Pependab L (2018) A new low-cost polymeric adsorbents with polyamine chelating groups for efficient removal of heavy metal ions from water solutions. *React. Funct. Polym.*

131: 64–74. <https://doi.org/10.1016/j.reactfunctpolym.2018.07.006>

[5] Jaishankar M, Tseten T, Anbalagan N (2014) Toxicity, mechanism and health effects of some heavy metals. *Interdiscip Toxicol.* 7(2): 60–72. doi: 10.2478/intox-2014-0009

[6] Ayangbenro AS, Babalola OO (2017) A New Strategy for Heavy Metal Polluted Environments: A Review of Microbial Biosorbents. *Int. J. Environ. Res. Public Health.* 14(1): 94. <https://doi.org/10.3390/ijerph14010094>

[7] Chételat J, Ackerman JT, Eagles-Smith CA, Hebert CE (2019) Methylmercury exposure in wildlife: a review of the ecological and physiological processes affecting contaminant concentrations and their interpretation, *Sci. Total Environ.* 711: 135117. <https://doi.org/10.1016/j.scitotenv.2019.135117>

[8] Aaseth J, Wallace DR, Vejrup K, Alexander J (2020) Methylmercury and Developmental Neurotoxicity: A Global Concern. *Current Opinion in Toxicology.* 19: 80-87. <https://doi.org/10.1016/j.cotox.2020.01.005>

[9] Engwa AG, Ferdinand PU, Nwalo FN, Unachukwu NM. (2019) Mechanism and Health Effects of Heavy Metal Toxicity in Humans. In: *Poisoning in the Modern World - New Tricks for an Old Dog.* <https://doi.org/10.5772/intechopen.82511>

[10] Jan AT, Azam M, Siddiqui K, Ali A, Choi I, Haq QM (2015) Heavy Metals and Human Health: Mechanistic Insight into Toxicity and Counter Defense System of Antioxidants. *Int. J. Mol. Sci.* 16(12): 29592-29630. doi: 10.3390/ijms161226183

[11] Islam A, Ahmad H, Zaidi N, Kumar S (2016) A graphene oxide decorated with triethylene-tetramine-modified magnetite for separation of chromium species prior to their sequential speciation and determination via FAAS. *Microchim. Acta*, 183:289 – 296. <https://doi.org/10.1007/s00604-015-1641-2>

[12] Ipeaiyeda AR, Ayoade AR (2017) Flame atomic absorption spectrometric determination of heavy metals in aqueous solution and surface water preceded by co-precipitation procedure with copper(II) 8-hydroxyquinoline. *Appl. Water Sci.* 7: 4449–4459. <https://doi.org/10.1007/s13201-017-0590-9>

[13] Martinis EM, Olsina RA, Altamirano JC, Wuilloud RG (2008) Sensitive determination of cadmium in water samples by room temperature ionic liquid based preconcentration and electrothermal atomic absorption spectrometry, *Anal. Chim. Acta.* 628: 41–48. <https://doi.org/10.1016/j.aca.2008.09.001>

[14] Wu P, Gao Y, Cheng G, Yang W, Lv Y, Hou X (2008) Selective determination of trace amounts of silver in complicated matrices by displacement-cloud point extraction coupled with thermospray flame furnace atomic absorption spectrometry, *J. Anal. At. Spectrom.* 23: 752–757. <https://doi.org/10.1039/B719579F>

[15] Khulbe KC, Matsuura T (2018) Removal of heavy metals and pollutants by membrane adsorption techniques. *Appl. Water Sci.* 8: 19. <https://doi.org/10.1007/s13201-018-0661-6>

[16] Vardhan KH, Kumar PS, Panda RC (2019). A review on heavy metal pollution, toxicity and remedial measures: Current trends and future perspectives. *J. Mol. Liq.* 290: 111197. <https://doi.org/10.1016/j.molliq.2019.111197>

[17] Renu, Agarwal M, Singh K (2017) Heavy metal removal from wastewater using various adsorbents: a review. *J. Water Reuse and Desalination*, 07(4): 387-419. <https://doi.org/10.2166/wrd.2016.104>

- [18] Diagboya PNE, Dikio ED (2018) Silica-based mesoporous materials; emerging designer adsorbents for aqueous pollutants removal and water treatment, *Micropor. Mesopor. Mater*, 266: 252-267, <https://doi.org/10.1016/j.micromeso.2018.03.008>.
- [19]. Da'na E (2017) Adsorption of heavy metals on functionalized-mesoporous silica: A review. *Microporous and Mesoporous Materials*, 247: 145-157. <https://doi.org/10.1016/j.micromeso.2017.03.050>.
- [20]. Lim J, Goh SS, Liow SS, Xue K, Loh XJ (2019) Molecular Gel Sorbent Materials for Environmental Remediation and Wastewater Treatment. *J. Mater. Chem. A*. **7**: 18759-18791. <https://doi.org/10.1039/C9TA05782J>.
- [21]. Huang W, Zhang Y, Li D (2017) Adsorptive removal of phosphate from water using mesoporous materials: A review, *Journal of Environmental Management*, Volume 193: 470-482. <https://doi.org/10.1016/j.jenvman.2017.02.030>
- [22]. Miller PJ, Shantz DF (2020) Amine-Functionalized Ordered Mesoporous Silicas as Model Materials for Liquid Phase Acid Capture. *AIChE Journal*. <https://doi.org/10.1002/aic.16918>
- [23]. Wamba AGN, Kofa GP, Koungou SN, Thue PS, Lima EC, Reis GS, Kayem JG (2018) Grafting of Amine functional group on silicate based material as adsorbent for water purification: A short review, *J. Environ. Chem. Eng.* 6: 3192-3203. <https://doi.org/10.1016/j.jece.2018.04.062>
- [24]. Hao Sh, Verlotta A, Aprea P, Pepe F, Caputo D, Zhu W. (2016) Optimal synthesis of amino-functionalized mesoporous silicas for the adsorption of heavy metal ions. *Microporous and Mesoporous Materials*, 236: 250-259. <https://doi.org/10.1016/j.micromeso.2016.09.008>
- [25] Wei J, Chen S, Li Y, He Z, Geng L, Liao L (2020) Aqueous Cu(II) ion adsorption by amino-functionalized mesoporous silica KIT-6. *RSC Adv.*, **10**, 20504-20514. <https://doi.org/10.1039/D0RA03051A>.
- [26] Saad R, Hamoudi S, Belkacemi K. (2008) Adsorption of phosphate and nitrate anions on ammonium-functionalized mesoporous silicas. *J Porous Mater.* 15: 315–323. <https://doi.org/10.1007/s10934-006-9095-x>
- [27]. Gupta R, Gupta SK, Pathak DD (2019) Selective adsorption of toxic heavy metal ions using guanine-functionalized mesoporous silica [SBA-16-g] from aqueous solution. *Microporous and Mesoporous Materials*, 288: 109577. <https://doi.org/10.1016/j.micromeso.2019.109577>.
- [28] Shahbazi A, Younesi H, Badiei A (2011) Functionalized SBA-15 mesoporous silica by melamine-based dendrimer amines for adsorptive characteristics of Pb(II), Cu(II) and Cd(II) heavy metal ions in batch and fixed bed column. *Chem. Eng. J. (Lausanne)* 168: 505–518. <https://doi.org/10.1016/j.cej.2010.11.053>
- [29] Kołodyńska D (2013) Application of a new generation of complexing agents in removal of heavy metal ions from different wastes. *Environ. Sci. Pollut. Res.* 20: 5939–5949. <https://doi.org/10.1007/s11356-013-1576-2>
- [30] Huang J, Ye M, Qu YQ, Chu LF, Chen R, He QZ, Xu DF (2012) Pb(II) removal from aqueous media by EDTA-modified mesoporous silica SBA-15, *J. Colloid Interface Sci.* 385 137–146. <https://doi.org/10.1016/j.jcis.2012.06.054>

- [31]. Zhao D, Huo Q, Feng J, Chmelka BF, Stucky GD (1998) Nonionic Triblock and Star Diblock Copolymer and Oligomeric Surfactant Syntheses of Highly Ordered, Hydrothermally Stable, Mesoporous Silica Structures, *J. Am. Chem. Soc.*, 7863: 6024–6036. <https://doi.org/10.1021/ja974025i>.
- [32] Brunauer JS, Emmet PH, Teller E (1938) Adsorption of Gases in Multimolecular Layers, *J. Amer. Chem. Soc.* 60: 309–319. <https://doi.org/10.1021/ja01269a023>
- [33] Barrett EP, Joyner LG, Halenda PP (1951) The Determination of Pore Volume and Area Distributions in Porous Substances. I. Computations from Nitrogen Isotherms, *J. Am. Chem. Soc.*, 73, 373–380. <https://doi.org/10.1021/ja01145a126>
- [34] Lin-Vien D, Colthup NB, Fateley WG, Grasselli JG (1991) In *The Handbook of Infrared and Raman Characteristic Frequencies of Organic Molecules*. Academic Press, London.
- [35] Han L, Ruan J, Li Y, Terasaki O, Che Sh (2007) Synthesis and Characterization of the Amphoteric Amino Acid Bifunctional Mesoporous Silica. *Chem. Mater*, 19 (11): 2860-2867. <https://doi.org/10.1021/cm0705845>
- [36] Zaitsev VN, Kobylinskaya NG (2005) Properties of silicas chemically modified by monodentate amines studied by conductometry. *Russ. Chem. Bull*, 54: 1842–1846. <https://doi.org/10.1007/s11172-006-0046-0>
- [37] Zhao D, Jing S, Xu J, Yang H, Zheng W, Song T, Zhang P (2013) Recycle adsorption of Cu²⁺ on amine-functionalized mesoporous silica monolithic. *Chem. Res. Chin. Univ.* 29: 793–797. <https://doi.org/10.1007/s40242-013-2442-y>
- [38]. Lever ABP (1974) Charge transfer spectra of transition metal complexes, *J. Chem. Educ.* 5: 612–616, <https://doi.org/10.1021/ed051p612>.
- [39] Smith RM, Martell AE (1987) Critical stability constants, enthalpies and entropies for the formation of metal complexes of aminopolycarboxylic acids and carboxylic acids. *Sci. Total. Envir*, 64(1-2): 125–147. [https://doi.org/10.1016/0048-9697\(87\)90127-6](https://doi.org/10.1016/0048-9697(87)90127-6).
- [40] Faghihian H, Naghavi M (2014) Synthesis of amine-functionalized MCM-41 and MCM-48 for removal of heavy metal ions from aqueous solutions. *Sep. Sci. Technol.* 49: 214–220.
- [41] Pearson RG (1963) [Hard and Soft Acids and Bases](#) *J. Am. Chem. Soc.* 85: 3533-3539. <https://doi.org/10.1021/ja00905a001>
- [42] Langmuir I (1918) The adsorption of gases on plane surfaces of glass, mica and platinum. *J. Am. Chem. Soc.*, 40(9): 1361–1403. <https://doi.org/10.1021/ja02242a004>
- [43] Freundlich HMF (1906) Über die adsorption in lasungen. *Z. Phys. Chem.* 57: 385–490. <https://doi.org/10.1515/zpch-1907-5723>
- [44] Dubinin MM (1960) The potential theory of adsorption of gases and vapors for adsorbents with energetically non-uniform surface. *Chem. Rev*, 60: 235-266. <https://doi.org/10.1021/cr60204a006>.

Figures

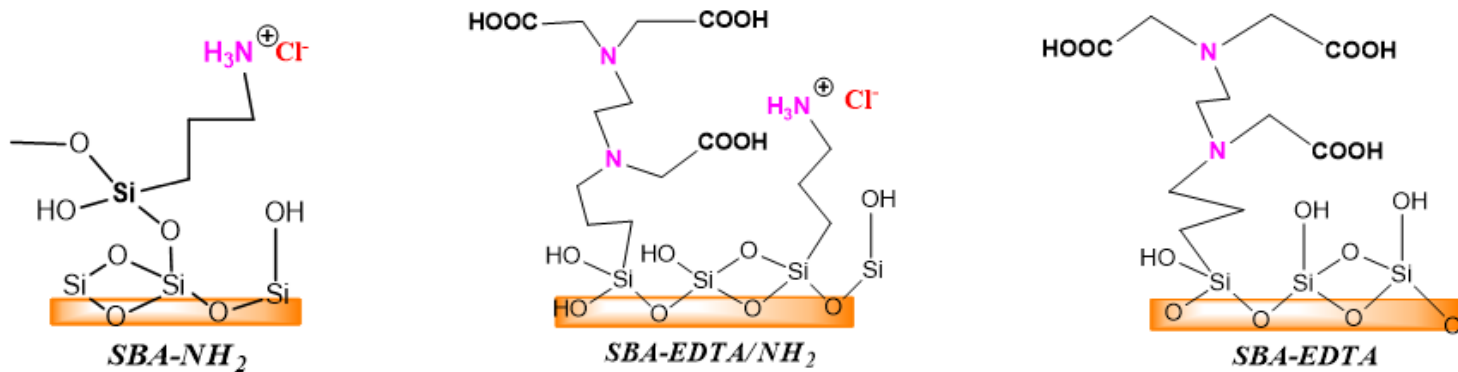


Figure 1

Surface layer and label of N-containing functional mesoporous silica.



Figure 2

TEM images of the SBA-NH₂ (a), SBA-EDTA/NH₂ (b) and SBA-EDTA (c) samples.

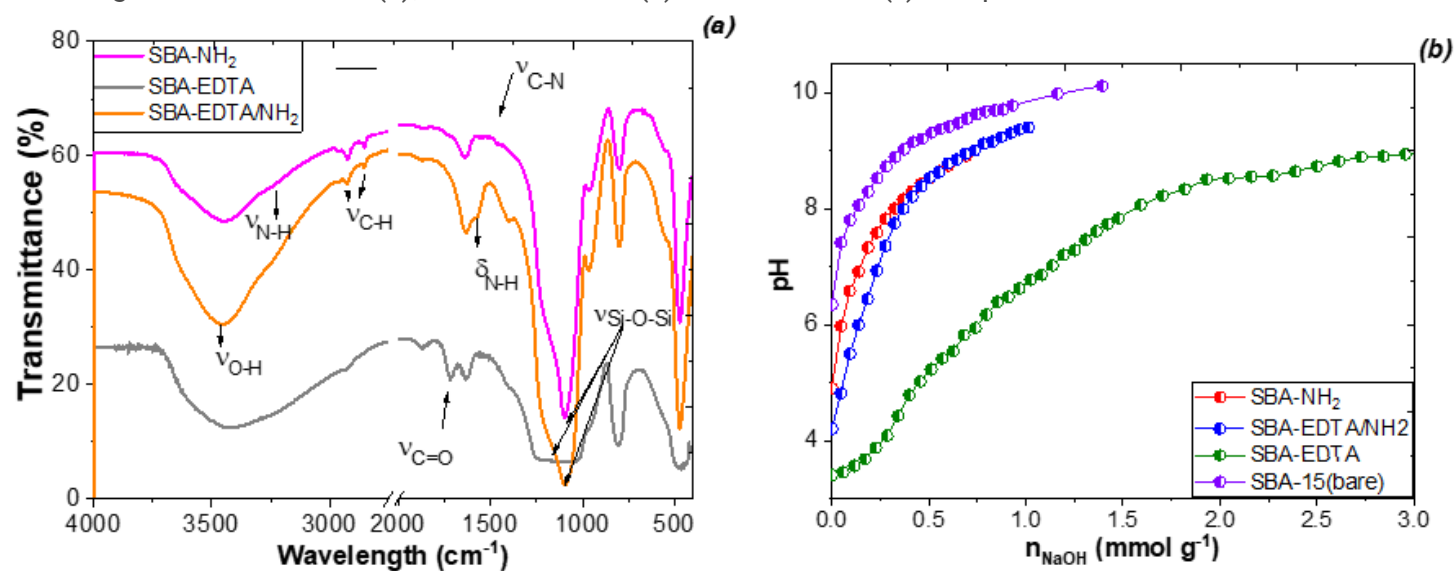


Figure 3

FTIR spectra (a) and titration curves (b) of the various silica samples.

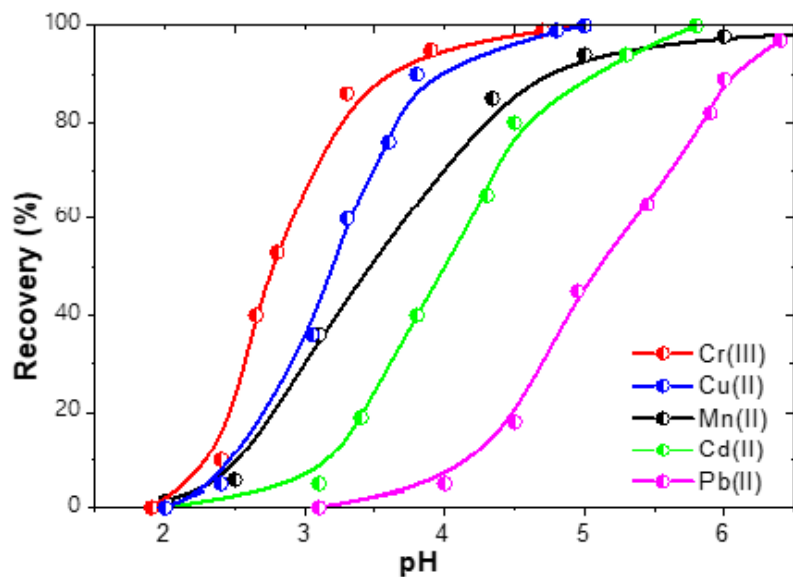


Figure 4

Recovery of metal ions on SBA-EDTA/NH₂ samples as a function of pH (Experimental conditions: CM= 2,5 10⁻⁵ mol L⁻¹, V=20 mL, m= 0.05 g, t = overnight).

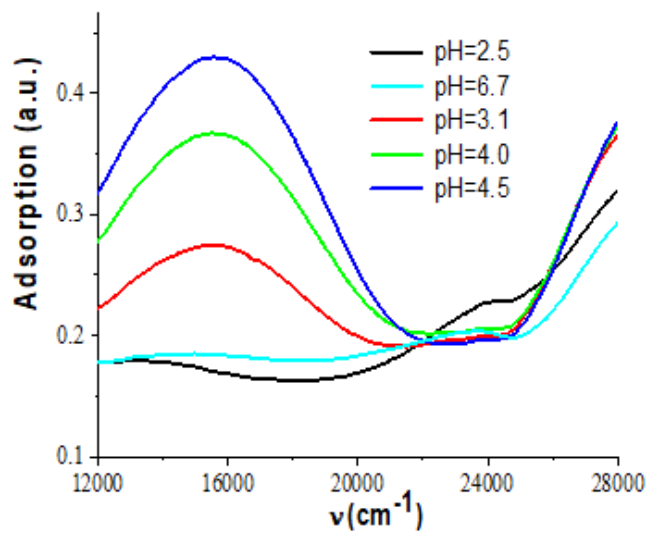


Figure 5

Diffuse reflectance spectra of SBA-EDTA/NH₂ samples after adsorption of Cu(II) ions with different pH.

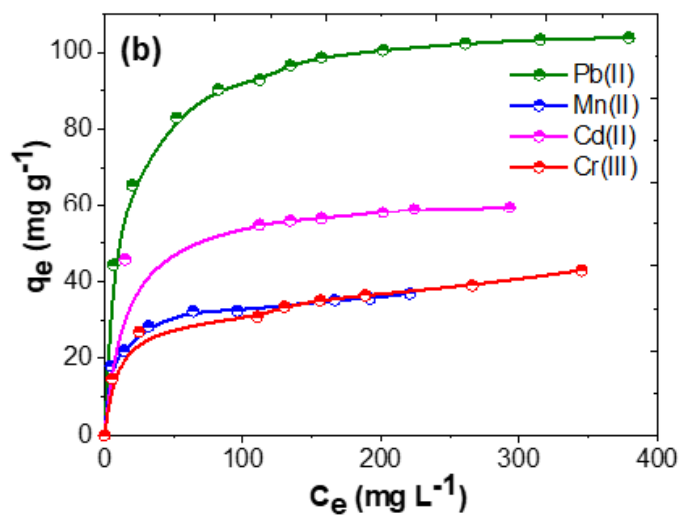
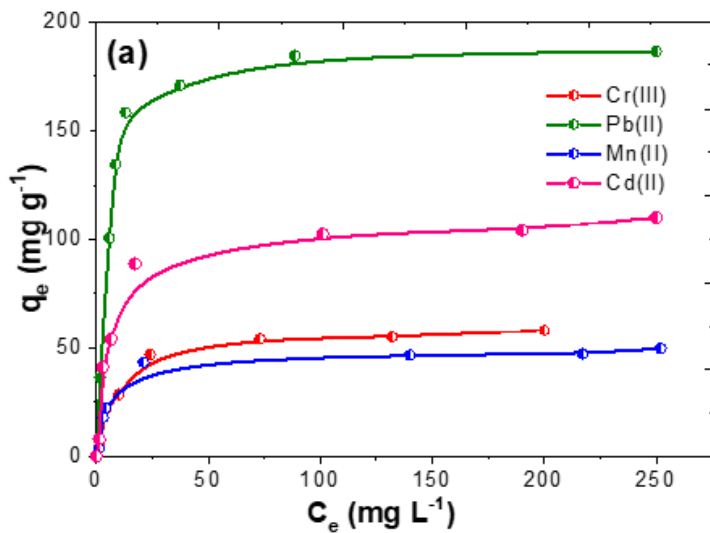


Figure 6

Sorption isotherms on SBA-EDTA (a) and SBA-EDTA/NH₂ (b) of metal ions: Cd(II) (pH = 5.8), 2 - Cr(III) (pH = 4.5), 3 - Mn(II) (pH = 5.5) and Pb(II) (pH = 6.0). (Experimental conditions: $m = 0.05$ g, $V = 25$ mL).

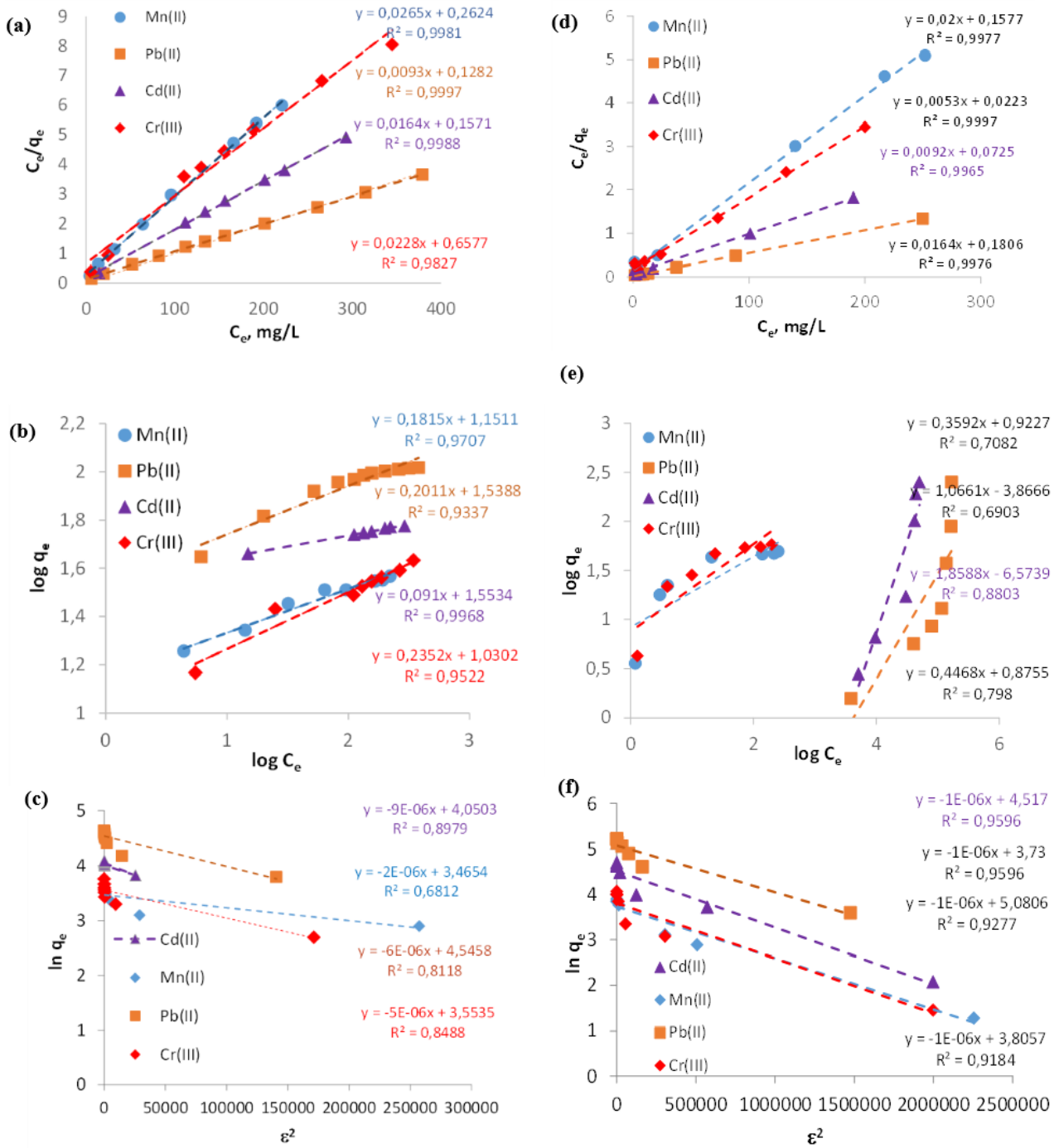


Figure 7

Langmuir (a, e), Freundlich (b, e) and Dubinin–Raduskevich (c, f) linearized form of adsorption of metal ions onto SBA-EDTA/NH₂ (a, b, c) and SBA-EDTA (d, e, f) samples.